A Non-Intrusive Impedance Cross-Correlation (ICC) Flow Meter for Dispersed Phase Velocity and Volume Fraction Profile Measurement in Two Phase Flows

Y.Muhamedsalih[1], G. P. Lucas[1],
[1] University of Huddersfield, Queensgate, Huddersfield HD1 3DH, UK

ABSTRACT

This paper describes the design and implementation of an impedance cross correlation flow meter which can be used in solids-water pipe flows to measure the local solids volume fraction distribution and the local solids velocity distribution. The system is composed of two arrays of electrodes, separated by an axial distance of 50 mm and each array contains eights electrodes mounted over the internal circumference of the pipe carrying the flow. Furthermore every electrode in each array can be selected to be either "excitation", "measurement" or "earth".
Changing the electrode configuration leads to a change in the electric field, and hence in the region of the flow cross section which is interrogated. The local flow velocity in the interrogated region is obtained by cross correlation between the two electrode arrays. Additionally, the local solids volume fraction can be obtained from the mean mixture conductivity in the region under interrogation. The system is being integrated with a microcontroller to measure the velocity distribution of the solids and the volume fraction distribution of the solids in order to create a portable flow meter capable of measuring the multi-phase flow parameters without the need of a PC to control it.
Integration of the product of the local solids volume fraction and the local solids velocity in the flow cross section enables the solids volumetric flow rate to be determined.

***Keywords**: Multiphase flow, cross-correlation, conductance sensors*

1. INTRODUCTION

The need for a reliable method, to measure multiphase flow parameters, was behind much reported research throughout the duration of the last century. Multiphase flow is the simultaneous flow of two or more phases in direct contact in a given system.
Separation technology now has a dominant role in the measuring process industries where large and expensive separators, are used to split the mixture into its various phases which are then metered them individually using single phase flow meters.
The rate at which a well is drilled and the rock cuttings volumetric flow rate Qcut should correspond to each other. If Qcut falls below the expected value this could indicate that cuttings are building up around the drilling assembly which could ultimately lead to the assembly becoming stuck in the well. In contrast if Qcut is greater than expected this could indicate that the well bore is collapsing, an occurrence that, if not corrected, will cost money and production time.

It is vital in many multiphase flow measurement applications to precisely monitor time averaged local volume fraction $\alpha_i$and the time averaged local velocity u_j of the j^{th} of the flowing phases to enable quantification of the flow rate Q_j of the j^{th} phase as follows:

$$Q_j = \int_A \alpha_j u_j d_A \tag{1}$$

Where: A is the cross section area.

2. IMPEDANCE CROSS CORRELATION FLOW METER

The Impedance Cross Correlation ICC flow meter described below is a modified version of an original design by Al-Hinai et al. (2010). This flow meter is used to determine the local solids volume fraction distribution and local solids velocity distribution in solids–liquid flows.

The ICC flow meter consists of two arrays of electrodes, separated by an axial distance of 50 mm and each array contains eights electrodes mounted over the internal circumference of the pipe

carrying the flow. Every electrode in each array can be selected to be either “excitation”, “measurement” or “earth”.

The ICC device has similar features of dual-plane electrical resistance tomography systems (ERT) because both techniques consist of two electrode arrays mounted around the pipe. Nevertheless, the ICC device has low implementation cost and needs no sophisticated algorithms to analyse the acquired data, in contrast to ERT systems. Additionally, the ERT systems need a PC station to control the system because the data analysis is based on generating conductivity images that are evaluated using sophisticated software packages. Opposed to ERT, the ICC can be integrated with a simple microcontroller to measure the velocity distribution of the solids and the volume fraction distribution of the solids. Al-Hinai (2010) also reported that values and spatial distributions of the local volume fraction obtained by EIT systems often do not follow the accepted pattern. Furthermore the mean volume fraction of the dispersed phase in an oil-water flow obtained using ERT differed markedly from the reference value obtained using a differential pressure measurement technique.

In the present study of solids-in-water flow, water which is the conductive phase is considered as the continuous phase while the solids are considered as the dispersed phase with zero electrical conductivity. Since the ICC flow meter has two electrodes arrays, two electrode selection circuits were designed to control the state for each electrode inside the array. The electrode selection circuits were designed to be able to select any electrodes from a given array (A or B) and connect them to excitation, measurement or to earth in the corresponding channel (A or B) of the conductance measurement circuit see AL-Hinai (2010). The switching mechanism allowed arrays A and B to be activated alternately. For the ICC device, in order to produce sensing regions inside the pipe, the states of each array are changed according to three defined configurations , These configurations can each be rotated (in steps of 45°) to eight rotational positions (n=1 to 8) to cover the measurements inside the cross section area of the pipe. These configurations are:

- Config. : in this configuration, one electrode is selected as excitation. The second electrode is selected as virtual earth measurement (ve). The remaining electrodes are selected as earth (E). For example, in rotational position-1, the electrode 1 is an excitation electrode and electrode 2 is the measurement electrode (ve), and electrodes 3,4,5,6,7 and 8 are connected to ground (E).
- Config. : in this configuration, one electrode is selected as excitation. Two electrodes are selected as virtual earth measurement (ve). The remaining electrodes are selected as earth (E). For example, in rotational position-1, electrode 1 is an excitation electrode, electrodes 8 and 2 are the measurement electrodes and the other five electrodes are connected to ground.
- Config. : in this configuration, two electrodes are selected as excitation, two electrodes are selected as virtual earth measurement (ve). The remaining electrodes are selected as earth (E). For example, in rotational position-1 electrodes 1 and 2 are the excitation electrodes, electrodes 3 and 8 are the measurement electrodes and the other four electrodes are connected to the earth (E).

Changing configurations gives rise to an Electrode Potential Rotational Pattern EPRP, which produces an effective sensing region $R_{\phi,n}$ (where ϕ or or corresponding to the different configuration described above and n 1 to).The effective sensing region has a centre of action CoA denoted $C_{\phi,n}$, with precisely defined coordinates and it is assumed that measured parameters associated with $R_{\phi,n}$ occur precisely at $C_{\phi,n}$. The boundary of the effective sensing region for each configuration at particular rotational position is located according to the sensitivity distribution results for that configuration (see Al-Hinai 2010), where the boundary is defined along the line where the sensitivity is 10% of the maximum sensitivity for the given electrode configuration.

In order to calculate the sensitivity distribution for each configuration and rotational position, a model of a „single plane’ of an -electode sensor has been produced in COMSOL using two dimensional finite element analysis. For a given plane the sensitivity of the sensing field of a given electrode configuration was calculated at numerous positions (or elements) in the flow cross section (Al-Hinai (2009)). In these simulations, the flow cross-section was assumed to be filled with water (the conducting medium) and material of zero conductivity was assumed to be inserted, in turn, into each element to simulate the presence of a non-conducting particle of the dispersed phase. The sensitivity parameter s_i for each element was calculated as follows:

$$s_i = (Vout)_0 - (Vout)_w \tag{2}$$

Where $(Vout)_0$ is the value of the output voltage when the element is at zero conductivity and $(Vout)w$ is the value of this output voltage when the element has the same conductivity as the water.

For example, Figure 2a illustrates the states of electrode and the effective sensing region for the first rotational position (n=1) for Config I. The pipe cross section area was divided into N elements with a side of length 2mm.For electrode configuration ϕ at rotational position n, the x co-ordinate for the "Centre of Action" for the effective sensing region in can be defined as:

$$(Cx)_{\phi,n} = \frac{\sum_{i=1}^{N} x_i a_i s_i}{\sum_{i=1}^{N} a_i s_i} \tag{3}$$

Where: $(Cx)_{\phi,n}$ is the x – co-ordinate of the CoA for Configuration ϕ and rotational position n, x_i is the distance in the x direction from the origin (centre of the pipe) to the i^{th} element in the COMSOL model, a_i is the area of the i^{th} element, s_i is the sensitivity parameter for the i^{th} element and N is the total number of elements in the flow cross-section. Similarly the y co-ordinate of the Centre of Action for configuration ϕ may be calculated from:

$$(Cy)_{\phi,n} = \frac{\sum_{i=1}^{N} y_i a_i s_i}{\sum_{i=1}^{N} a_i s_i} \tag{4}$$

Where: $(Cy)_{\phi,n}$ is the y– co-ordinate of the CoA for Configuration ϕ and rotational position n, y_i is the distance from the origin (centre of the pipe) to the i^{th} element in the COMSOL model on the y-axis. By repeating the same steps for Config. and Config. , the coordinates of 24 different centres of action were calculated as shown schematically in Figure 3.

3. CONDUCTANCE CIRCUIT DESIGN

A conductance circuit has been designed in order to measure the conductance of the multiphase mixture between the V+ and ve electrodes, sequentially for each of the eight rotational positions, for a given configuration. The excitation V+ electrodes are connected to s1 in figure 4 and the ve electrodes are connected to s2, and E electrodes are grounded. For a given configuration and rotational position connection of the V+ electrodes to s1, the ve electrodes to s2 and the E electrodes to ground was undertaken using an electrode selection circuit described in section 2.1. s1 can be one electrode or more depending on the chosen configuration. It is connected to the sinusoidal signal with a 10 Khz frequency while s2 (where s2 also can be one electrode or more depending on the chosen configuration) is connected to the negative input for the inverting amplifier as shown in Figure 4. Figure 4 shows the conductance fluid circuit which used to measure the change in the conductivity of the flow inside the pipe, where Rf is the fluid resistance between the excitation electrodes and the virtual earth electrodes and R2 is the feedback resistance for the inverting amplifier. R_y is the fluid resistance between the excitation electrode and the grounded electrodes, while R_x is the fluid resistance between the virtual earth electrode and the grounded electrodes.Since R_y has no effect on the operation of the amplifier, the current equation of the conductance circuit can be written as:

$$I_2 = I_1 + I_x + I_{in} \tag{5}$$

Where: I_2 is the feedback current, I_1 is the current between the $V(t)$ and ve, I_x is the current between the ve and the ground and I_{in} is the internal amplifier current. The ve voltage can be given as:

$$ve = \frac{-Vout}{A} \tag{6}$$

Where: A is the open loop amplifier gain.
We can re-write equation 5 in term of the voltages and resistances as follows:

$$\frac{Vout+(Vout/A)}{R_2}=\frac{-(Vout/A)-(V(t))}{R_f}+\frac{-(Vout/A)}{R_{in}}+\frac{-(Vout/A)}{R_x} \tag{7}$$

$$Vout[\frac{1}{R_2}+\frac{1}{AR_2}+\frac{1}{R_f}+\frac{1}{AR_{in}}+\frac{1}{AR_x}]=\frac{-(V(t))}{R_f} \tag{8}$$

The relation between *Vout* and *V(t)* can be shown in equation (8):

$$\frac{Vout}{V(t)}=-\frac{R_2}{R_f}\left\{\frac{1}{1+\frac{1}{A}(1+\frac{R_2}{R_f}+R_2\left(\frac{1}{R_{in}}+\frac{1}{R_x}\right))}\right\} \tag{9}$$

When the open loop gain (A) is very high, (which is the case for the LF356 amplifier used in the present study) equation (9) can be simplified to give

$$\frac{Vout}{V(t)}=-\frac{R_2}{R_f} \tag{10}$$

And so the fluid resistance R_x in Figure 5 can be ignored.

Consideration of equation 10 enables the conductivity $(\sigma_m)_{\phi,n}$ between the $V(t)$ and ve electrodes to be written as:

$$(\sigma_m)_{\phi,n}=K_{\phi,n}|V(t)| \tag{11}$$

Where: $|V(t)|$ represents the amplitude of the input sine wave $V(t)$ and where $K_{\phi,n}$ is a „cell constant' for configuration ϕ and rotational position n. The local mixture conductivity (of a region of the flow containing a „representative' concentration of solid particles) can be used to make an estimate the local solids volume fraction $(\alpha_d)_{\phi,n}$ by invoking the following simplified from Maxwell's equation for the conductivity of mixture see(Cory 1999):

$$(\alpha_d)_{\phi,n}=\frac{2\sigma_w-2(\sigma_m)_{\phi,n}}{(\sigma_m)_{\phi,n}+2\sigma_w} \tag{15}$$

Where: σ_w is the electrical conductivity of the water, and the corresponding local volume fraction of the water in each interrogated region is $1-(\alpha_d)_{\phi,n}$.

The conductance circuit described above has been designed to apply these arrangements to arrays A and B in such a way that the conductivities $(\sigma m)_{\phi,n,A}$ and $(\sigma m)_{\phi,n,B}$ from both planes A and B were obtained. In order to control the excitation signal $V(t)$ which supplies the two arrays, a switching mechanism has been used, where a signal generator XR-2206 is used to produce a high quality pulse waveforms of high-stability and accuracy. The purpose of using the XR-2206 is to ensure that the $V(t)$ electrodes in array A and the $V(t)$ electrodes in array B were connected alternately to the excitation source. This meant that planes A and B were never active at the same time and so prevented „cross talk' between the two planes. The switching frequency was 110 kHz while the excitation signal applied to the $V(t)$ electrodes was 10 KHz. The results of the applied signals to channel A and B could be shown in Figure 5. The output signals from the channel A (array A) and channel B (array B) were passed through a low pass filter in order to remove any high frequency noise. Additionally the both signals were rectified and low pass filtered to produce d.c. output voltages $VA_{\phi,n}(t)$and $VB_{\phi,n}(t)$ which could be subsequently cross correlated to provide information on the local dispersed phase velocity of a two phase flow at the particular region of the flow cross section „interrogated' at planes A and B.

The cross correlation function for the dispersed phase in each interrogated region can be calculated as:

$$R_{\phi,n}(\tau)=\frac{1}{T}\int_0^T VA_{\phi,n}(t)\,VB_{\phi,n}(t+\tau)dt \tag{12}$$

Where ϕ is the configuration type, n is the rotation number, $VA_{\phi,n}(t)$ is the output voltage from channel A at time t, $VB_{\phi,n}(t+\tau)$ is the output voltage from channel B at time $(t+\tau)$, τ is the delay time and T is the total time period for which data acquired. As the delay time τ varies from 0 to the total time period T, the value of cross correlation function $R_{\phi,n}(\tau)$ will change, attaining a maximum value when τ is equal to τ_p the mean time for the perturbations in the relevant property of the flow to travel

from array A to array B. Thus, τ_p can be found by determining the value of τ at which $R_{\phi,n}(\tau)$ is a maximum. The local velocity in each interrogated region can be determined by:

$$(u_d)_{\phi,n} = \frac{}{(\tau_p)_{\phi,n}} \quad (13)$$

Where: $(u_d)_{\phi,n}$ is the local solids velocity at configuration ϕ and rotation n, L is the axial distance between arrays A and B. The distributions of the local solids volume fraction and local axial velocity obtained by the ICC flow meter can be used to estimate the solids volumetric flow rate, as shown in the following equation:

$$Q_d = \sum_{i=1}^{N} (\alpha_d)_{\phi,n} (u_d)_{\phi,n} A_n \quad (16)$$

Where: A_n is the interrogated cross section area.

4. FLOW LOOP TESTING OF THE ICC SYSTEM

The ICC flow meter was mounted in an inclinable multiphase flow loop (Cory 1999) for testing in solids-in-water flows inclined at 15˚ and 30˚ to the vertical. The measurement techniques described above were implemented in order to determine the local solids volume fraction distribution and local axial solids velocity distribution in the cross-section for various flow conditions. Figure 6(a) shows the interpolated local volume fraction distribution for 15˚ pipe inclination to the vertical, a water volumetric flow rate Q_w equal to 10.91 m3 h-1 (cubic metres per hour) and a solids volumetric flow rate Q_d of 0.73 m3 h-1 . Figure 6(b) shows the interpolated local volume fraction distribution for 30˚ inclination to the vertical, for Q_w equal to 10.79 m3 h-1 and Q_d equal to 0.591 m3 h-1 . Config I was used in both cases. It is clear from figure 8 that the local solids volume fraction at the lower side of the inclined pipe increases rapidly with increasing pipe inclination angle to the vertical.

Figure 9 shows distributions of the local axial solid velocity u_d for solids-in-water flows inclined at 15˚ and 30˚ to the vertical. Figure 7(a) (15˚) shows the interpolated distribution of u_d for Q_w equal to 9.45 m3 h-1 and Q_d equal to 0.613 m3 h-1 . Figure 7(b) (30˚) shows the interpolated distribution of u_d for Q_w equal to 10.79 m3 h-1 and Q_d equal to 0.591 m3 h-1 . Config. I was again used in both cases. For inclined upward flow, the distribution of the measured local axial solids velocity u_d is highly non-uniform with the solids velocity varying from a minimum value at the lower side of the inclined pipe to a maximum value at the upper side. It is clear from figure 9 that the rate at which the changes in u_d occur increases sharply with increasing pipe inclination angle to the vertical.

It should be noted that the mean solids volume fraction and mean solids velocity obtained from the data presented in figures 6 and 7 gave good agreement with reference measurements of these quantities. These reference measurements were made using techniques described in detail in AL-Hinai (2010).

5. CONCLUSIONS

An ICC device has been designed and built which interrogates separate regions of the flow cross section. In a two phase flow in which the continuous phase is electrically conducting and where the dispersed phase has much lower conductivity it is possible to determine the „local' volume fraction of both phases in each region and the „local' axial velocity of the dispersed phase in each region. These measured values are assumed to apply at the Centre of Action (CoA) of each region, the position of which has been calculated using COMSOL software. By integrating the product of the dispersed phase volume fraction and the dispersed phase velocity in the flow cross section it will be possible to estimate the volumetric flow rate of the dispersed phase. To date, simple bench tests have been carried out on the ICC in order to evaluate control of the device using a VM1 microcontroller. The next stage is to measure volume fraction and velocity profiles in highly non-uniform multiphase flows.

The major advantage of the ICC approach, as opposed to more usual Electrical Resistance Tomography methods, is that no image reconstruction algorithms need to be employed. It has been found by the authors of the present paper that the image reconstruction algorithms used in many ERT systems can introduce significant errors, particularly in the measured local volume fraction distributions.

6. REFERENCES

Hewitt G., Delhaye J., Zuber N., 1986, Multiphase science and Technology, Volume 2, Hemisphere Publishing Corporation.

Lucas G., et al, 1999, Measurement of the solids volume fraction and velocity distributions in solids-liquid flows using dual-plane electrical resistance tomography, University of Huddersfield, UK.

Al-Hinai, Lucas, (2009), A flow meter of measuring the dispersed phase velocity in multiphase flow with non-uniform profiles, vol.9. Journal of JSEM.

Beck M., Plaskowski A., 1987, Cross correlation flowmeters – their design and application, IOP Publishing Ltd.
X Deng, F Dong, L J Xu, X p Liu and LA Xu (2001), the design of a dual-plane ERT system for cross correlation measurement of bubbly gas/liquid pipe flow.

Cory J., 1999, The Measurement of Volume Fraction and Velocity Profiles in Vertical and Inclined Multiphase Flows, University of Huddersfield, UK.

AL-Hinai, 2010, Non-Invasive Velocity and Volume Fraction Profile Measurement in Multiphase Flows, University of Huddersfield, UK.

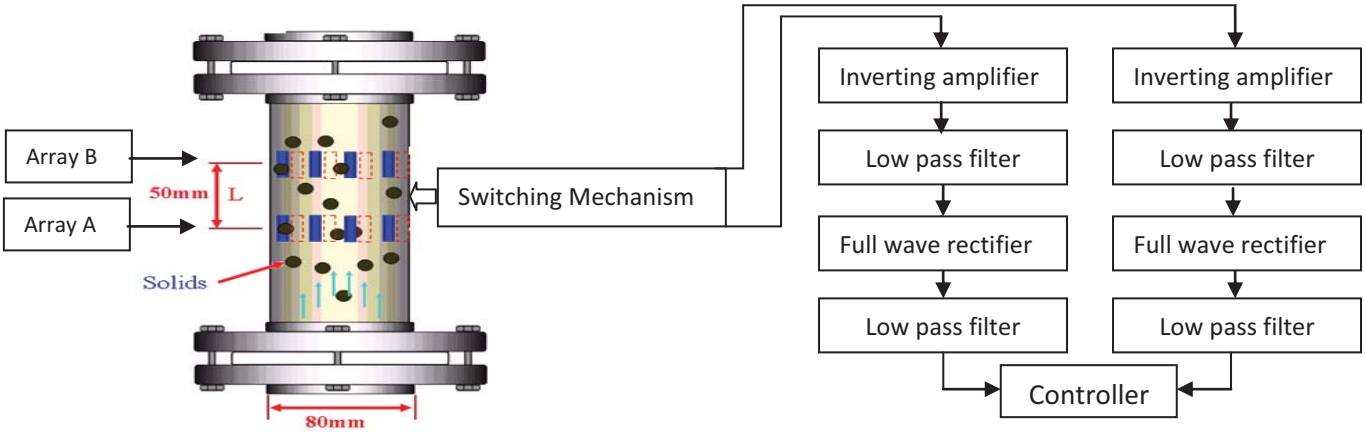

FIGURE 1. Schematic diagram for the ICC flow meter

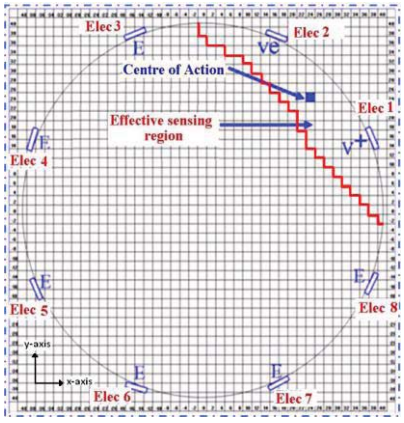

FIGURE 2. Effective sensing regions associated with Config-I, rotation 1. AL-Hinai (2010)

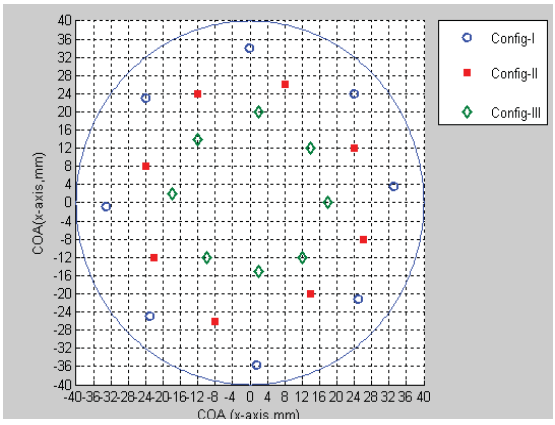

FIGURE 3. Location of CoA for Config-I, II and III for each of the eight possible electrode rotational positions per configuration. AL-Hinai (2010)

.

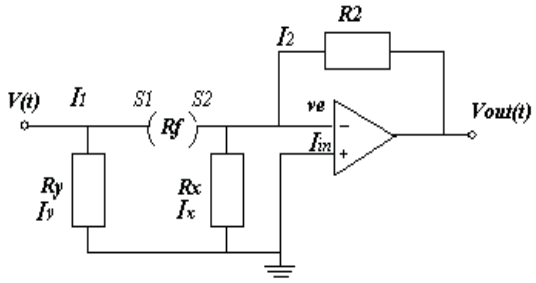

FIGURE 4. the conductance fluid circuit

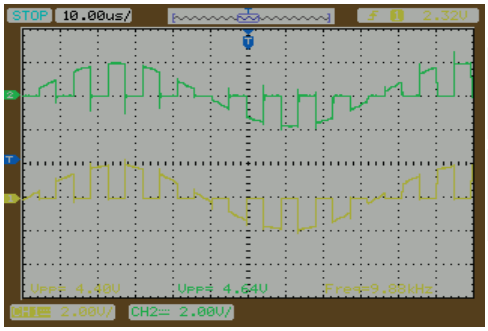

FIGURE 5. the excitation signals in array A and B

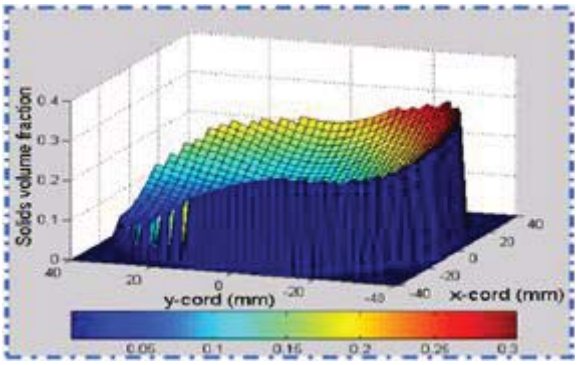

(a) Flow inclined 15˚ from vertical

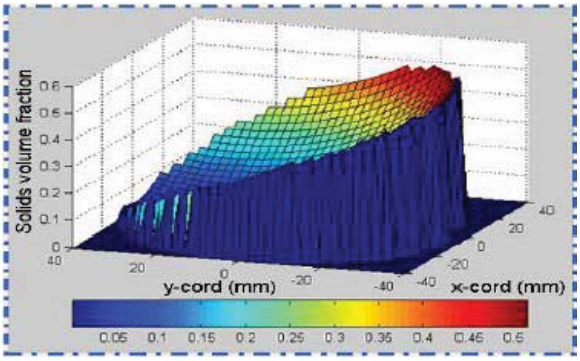

(b) Flow inclined 30˚ from vertical

Figure 6. 3D Profiles of the local solids volume fraction from the ICC

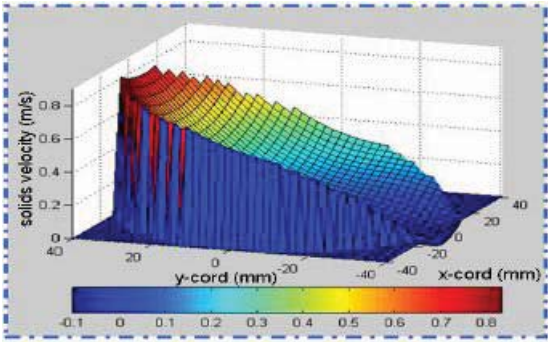

(a) Flow inclined 15˚ from vertical

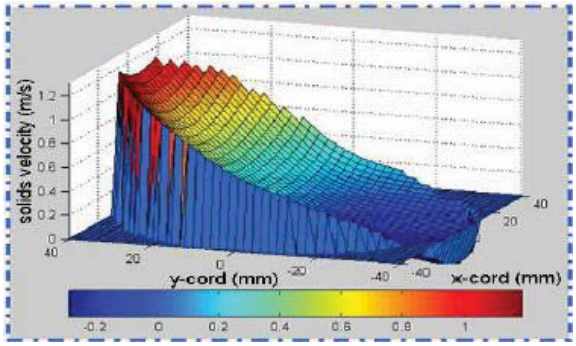

(b) Flow inclined 30˚ from vertical

FIGURE 7. 3D Profiles of the local solids velocity from ICC